Development of an Electrophotographic Laser Intensity Modulation Model for Extrinsic Signature Embedding

Pei-Ju Chiang[1], Aravind K. Mikkilineni[2], Edward J. Delp[2], Jan P. Allebach[2] and George T.-C. Chiu[1]
School of Mechanical Engineering[1], School of Electrical and Computer Engineering[2]
Purdue University; West Lafayette, Indiana/USA

Abstract

In our previous work, we have demonstrated techniques to embed and extract extrinsic signatures from halftone images and text documents. Well developed embedding algorithms should increase the payload capacity while enhance the reliability of detection. In this study, we will develop a printer model that will be used to optimize the embedding algorithm for capacity and detection reliability. The model incorporates the impact of the process modulation parameter, e.g. laser intensity, with a stochastic dot interaction model to estimate the impact of the modulation on a known halftone pattern. Experimental data validated the effectiveness of the proposed model in predicting the impact of laser intensity modulation on the reflectance of the printout.

Introduction

Printer identification based on a printed document can provide forensic information to protect copyright and verify authenticity. In our previous work [1,2], we have demonstrated the feasibility of modulating dot gains through laser intensity modulation for halftone images and text document to embed unperceivable code sequences. To optimize the embedding and detections algorithms, significant amount of printing and measurements are needed. To reduce the time and effort, a suitable electrophotographic (EP) process model that characterizes the impact of laser intensity modulation on the printed image will be needed. In particular, a computation efficient model that characterizes the dot interactions among the printed pixels in a halftone pattern is a key component.

Several dot interaction models for the EP process have been proposed in the literature. Roetling and Holladay [3] proposed the hard circular dot (HCD) model to account for spreading of colorant on the substrate that causes increased absorptance of the print. In this model, each printer addressable dot is assumed to be a circular spot with constant absorptance, and dots overlap are resolved by a logical OR at each point in the print. Pappas et al. [4] parameterized the HCD model and proposed a method to obtain the printer model parameters through macroscopic measurements of the test patterns [5]. Rosenberg [6] used HCD model to predict the tone response of various halftone algorithms and compensates the monotonic printer distortions before halftoning. Baqai and Allebach [7] incorporated the HCD model into the direct binary search (DBS) halftone algorithm to minimize the perceived mean-square error between the halftoned image and the continuous-tone image. To account for the dot scatter in EP process, Lin and Wiseman [8] proposed a stochastic dot model to model the toner particles distribution on addressable dots. Lin [9] used this model

to improve the pattern uniformity and tonal response of frequency modulated halftone screens. Flohr et al. [10] also used a similar stochastic dot model to improve the halftone image quality produced by DBS.

In this work, we will modify Lin's [8] stochastic model to include the effect of laser intensity modulation used for extrinsic signature embedding to predict the reflectance of the printout. Using the proposed model, modulation threshold of various embedding algorithms can be efficiently estimated with fewer measurements. In addition, the modulation signal can be optimized to enhance the capacity and detection reliability through feedback of the estimated values. In this study, an HP Color Laserjet 4500 is used as the experimental platform.

The remainder of this paper is organized as follows. Characterization of laser intensity modulation is discussed in the next section followed by the development of the stochastic dot interaction model with laser intensity modulation. Preliminary experimental results will be presented. Conclusions will be summarized in the last section.

Characterization of Laser Intensity Modulation

The intensity profile of the laser is modeled as a 2-D Gaussian envelope given by.

$$I(x,y,t) = I_0(t) \cdot \exp\left(-\frac{y^2}{2\alpha^2} - \frac{x^2}{2\beta^2}\right) \quad \left[W/m^2\right] \quad (1)$$

where $I_0(t)$ represents the power amplitude of the laser. α and β are the standard deviations of the Gaussian laser beam profile in the process (y) and scan (x) directions, respectively. If the laser is switched on at time 0 and off at time t_{off} and assuming exponential rise and fall transitions, the transient laser power amplitude can be expressed as

$$I_0(t) = \begin{cases} 0, & t < 0 \\ I_{max}\left[1 - \exp\left(-\frac{t}{t_r}\right)\right], & 0 \le t \le t_{off} \\ I_{max}\left[1 - \exp\left(-\frac{t_{off}}{t_r}\right)\right] \cdot \exp\left(\frac{-(t - t_{off})}{t_f}\right), & t > t_{off} \end{cases} \quad (2)$$

where I_{max} is the full value of laser power. Let the nominal values of the printed pixel width in the scan and process directions be X and Y, respectively. Assume the laser beam translates along the scan (x) direction at a linear velocity V that is significantly higher compared to the linear velocity of the photoconductor surface. The exposure energy at any arbitrary point (x, y) due to the pixel [m,n] with center (x_m, y_n) being turned on is found by integrating Eq. (2) with respect to time as:

$$E_{mn}(x, y) =$$

$$\int \left[I_0(t) \cdot \exp\left(-\frac{(y - y_n)^2}{2\alpha^2} - \frac{(x - (x_m - X/2) - Vt)^2}{2\beta^2} \right) \right] dt \ \left[J/m^2 \right], \quad (3)$$

Impact of Laser Intensity Modulation - Dot Size

When I_{max} increases, the laser power $I_0(t)$ and the exposure energy also increase. Since the laser power is proportional to the laser diode current that is proportionally controlled by the laser intensity V_r, the peak laser power I_{max} can be modeled to be proportional to V_r as

$$I_{max} = \gamma \cdot V_r \quad \left[W/m^2 \right], \quad (4)$$

where γ is the proportional constant between I_{max} and V_r.

Figure 1(a) shows the average dot profile of 16 dots when V_r is held constant at 1.1, 1.3, 1.5 and 1.7 volts for the experimental system. Figure 1(b) shows the relationship between the input laser intensity in volts and dot sizes. The dot size is determined by counting the number of pixels with an absorptance value greater than 0.1 in one dot cell scanned with a 8000 dpi drum scanner. As input voltage increases, dot size increases.
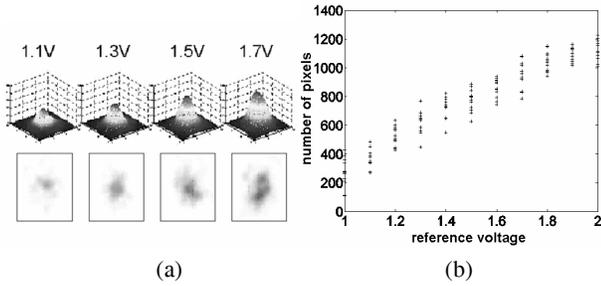

(a)   (b)

Figure 1. *(a) dot profiles for different reference voltage V_r (b) Dot size versus V_r*

Impact of Laser Intensity Modulation - Dot Shift

In addition to a proportional change in the corresponding dot size, modulating laser intensity also introduces a shift in each scanline. Figure 2 shows the effect of scanline shift due to laser intensity modulation. The letter I in Fig. 2(a) is printed without any modulation while the letter I in Fig. 2(b) is printed with a 40 cycles/in square wave laser intensity modulation. The existence of the embedded signal and a horizontal dot shift are clearly seen in Fig. 2(b). The dot shift is due to the change in the trigger timing of the beam detection signal used to signal the beginning of each scanline when the laser intensity is modulated by V_r. If the laser intensity is higher, the corresponding laser intensity profile will get wider and the triggering of the beam detect signal will occur earlier as shown in Fig. 2(c). Since laser intensity is modulated per scanline, the pixels in the same scanline will shift by the same distance in the scan (x) direction.

Let the threshold of beam detection be I_{th}. The amount of dot shift (Δx) between the laser intensity modulated by V_r and the nominal intensity V_0 can be calculated by

$$\Delta x(V_r) = \sqrt{-2\beta^2 \cdot \ln\left(\frac{I_{th}}{I_{max}(V_r)} \right)} - \sqrt{-2\beta^2 \cdot \ln\left(\frac{I_{th}}{I_{max}(V_0)} \right)} \quad (5)$$
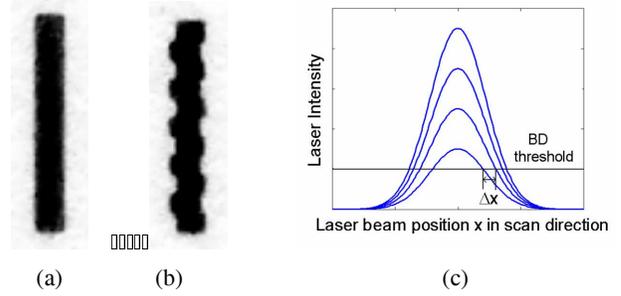

(a)   (b)   (c)

Figure 2. *(a) Letter I printed without modulation (b) Letter I printed with 40 cycles/in square wave laser intensity modulation (c) Laser dot profiles in scan direction x with various laser power intensity*

Experiments are conducted to measure the amount of dot shift as a function of the laser intensity V_r. A test page composed with three lines of dots is printed at the printer resolution. The first and the third line of dots are printed with laser intensity $V_r = 2.0$ and the second line is printed with $V_r = 1.0, 1.1, ... , 1.9$ volts, respectively. The printed pages are scanned at 8000 dpi with a calibrated Aztek Premier drum-scanner. The scanned dot patterns are shown in Fig. 3. A binary segmentation mask image produced by the scanned image is utilized to find the cell boundary for each dot. Within the $M \times N$ cell of the original gray image, the center point of each dot (C_{xi}, C_{yi}) is calculated by

$$C_{x_i} = \frac{\sum_{n=1}^{N} \sum_{m=1}^{M} R_{m,n} x_{im}}{\sum_{n=1}^{N} \sum_{m=1}^{M} R_{m,n}}, \quad (6)$$

$$C_{y_i} = \frac{\sum_{n=1}^{N} \sum_{m=1}^{M} R_{m,n} y_{in}}{\sum_{n=1}^{N} \sum_{m=1}^{M} R_{m,n}}, \quad (7)$$

where i is the index of the dot, $R_{m,n}$ is the reflectance value of the image at the pixel with coordinates (x_{im}, y_{in}). The shift distance can be calculated by

$$d = \frac{\left| (C_{x_2} - C_{x_1})(C_{y_1} - C_{y_0}) - (C_{x_1} - C_{x_0})(C_{y_2} - C_{y_1}) \right|}{\sqrt{(C_{x_2} - C_{x_1})^2 - (C_{y_2} - C_{y_1})^2}}, \quad (8)$$
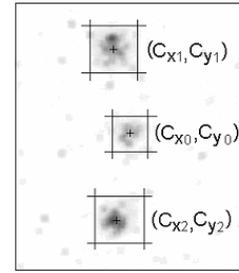

Figure 3. *8000 dpi scan of 3 lines of dots rendered with an HP LaserJet 4500 printer at 600 dpi. The first and the third line is modulated with Vr = 2.0 volt and the second line is modulated with Vr = 1.0 volt*

For each laser intensity value V_r, ninety sets of dot configurations are printed and measured. Since $V_0 = 1.5$ is the nominal intensity, let the shift distance associated with the laser intensity $V_r = 1.5$ be zero. The mean values of measured dot shift according to different modulation intensity are given in Fig. 4. As shown in Fig. 4, the relationship between dot shift Δx and laser intensity V_r can be fitted by an exponential curve

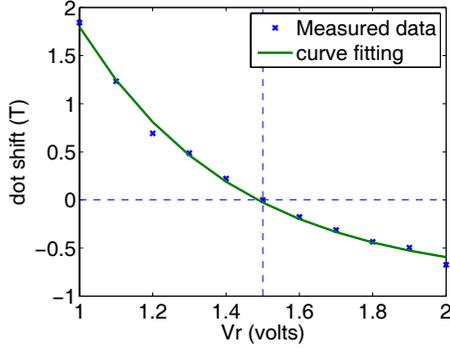$$\Delta x(V_r) = k_1 \cdot e^{-(k_2 \cdot V_r)} + k_3 . \qquad (9)$$

Figure 4. Dot/Scanline shift associated to various laser intensity V_r

Stochastic Dot Model

Lin and Wiseman [8,9] proposed a stochastic dot model that treats the probability of a toner particle being developed at a particular location as a Gaussian distributed around the center of the dot. As shown in Figs. 1(a) and 2(c), different laser intensity induces different exposure energy and dot size/gain. It is reasonable to assume that the toner distribution associated with the stochastic dot model is also a function of laser intensity V_r. Assume all toner particles are identical in size and shape, then each addressable pixel (i, j) with area $T \times T$ inch^2 is divided into $U \times V$ lattice cells for placement of toner particles. The coordinate $(x_{i,u}, y_{j,v})$ of the toner particle at u^{th} row and v^{th} column in the lattices of pixel (i, j) is given by

$$\begin{cases} x_{i,u} = [(i-1)U + u] \cdot du - du/2 \\ y_{j,v} = [(j-1)V + v] \cdot dv - dv/2 \end{cases}, \qquad (10)$$

where $du = T/U$ and $dv = T/V$.

Assume the image is half-toned with a binary array $b_{m,n}$, where $b_{m,n} = 1$ denotes that a dot is printed at pixel (m, n) and $b_{m,n} = 0$ denotes that no dot is printed. Let $t(x_{i,u}, y_{j,v}) = \{0,1\}$ be a random variable indicating whether a toner particle is placed at lattice coordinate $(x_{i,u}, y_{j,v})$, where $t(x_{i,u}, y_{j,v}) = 1$ indicates toner particles are placed and $t(x_{i,u}, y_{j,v}) = 0$ indicates no toner particle is placed. The probability density function of toner distribution, i.e. $t(x_{i,u}, y_{j,v}) = 1$, for pixel (m, n), is given by

$$p = \Lambda(V_r) \cdot e^{-\mu d^2} , \qquad (11)$$

where Λ is the intensity of toner distribution which is between 0 and 1 depending on the laser intensity V_r, μ is an indicator of dot scattering and d is the distance between the toner particle and addressable pixel center (x_m, y_n) calculated by

$$d = \sqrt{(x_{i,u} - x_m - \Delta x)^2 + (y_{j,v} - y_n)^2} . \qquad (12)$$

In this model, dot interaction is accounted for by the logical OR of toner distribution from adjacent pixels. The area covered with toner from the addressable lattice area $T \times T$ inch^2 at pixel location (i, j) can be presented as follow:

$$A_{i,j} = \frac{1}{T^2} \sum_{u=1}^{U} \sum_{v=1}^{V} \bigcup_{m,n} b_{m,n} \cdot t(x_{i,u}, y_{j,v}) du dv , \qquad (13)$$

To estimate the density D_t of the printout, the Yule-Nielsen equation

$$D_t = -n \cdot \log\left[(1-A)10^{-D_0/n} + A \cdot 10^{-D_s/n} \right], \qquad (14)$$

where A is the area covered with toner, D_s is the solid colorant density, D_0 is the paper density without any colorant, n is the Yule-Nielsen factor used to account for the dot gain, is applied. Using R to represent the reflectance of the printout, where $D = -\log(R)$, Yule-Nielsen equation can be re-written in terms of reflectance as

$$R_t = \left[(1-A)R_0^{1/n} + AR_s^{1/n} \right]^n , \qquad (15)$$

Experimental Results

To verify the laser intensity modulation model, we will compare the reflectance of a printed halftone image with the reflectance predicted by the model under different intensity modulation. A gray patch with 50% fill is rendered using a 8×8 clustered dot dither algorithm. Each addressable dot is divided into 50×50 lattice for placement of toner particles. The total area filled with toner particles in one pixel is calculated according to Eq. (13). Based on the Yule-Nielsen equation, Eq. (15), the mean reflectance for each pixel in the halftone screen can be estimated. For comparison, a test page with the same halftone screen is printed and the mean reflectance for each pixel in the halftone screen is also measured using a calibrated flatbed scanner. Model parameters Λ and μ in Eq. (11) and the Yule Nielsen factor n in Eq. (15) are obtained by minimizing the sum of squared difference between the estimated and the measured reflectance of each pixel in the halftone screen. The sum of square error C_1 between the estimated and the measured reflectance for a specific laser intensity laser intensity V_r is given by

$$C_1(n, V_r, \Lambda, \mu) = \sum_c (\bar{R}(c, V_r) - \hat{R}(c, n, \Lambda, \mu))^2 , \qquad (16)$$

where c is the cell index in the halftone screen, $\bar{R}$ is the estimated mean reflectance in one cell, and $\hat{R}$ is the measured one. The best fit Λ for specific n and μ with laser intensity V_r is given by

$$\Lambda_b(n, V_r, \mu) = \arg\min_{\Lambda} C_1(n, V_r, \Lambda, \mu) . \qquad (17)$$

Similarly, the optimum selection of the pair of (n, μ) to minimize the maximum error among all laser intensity V_r with Λ_b is

$$(n, \mu)_{opt} = \arg\min_{n, \alpha} \left\{ \max_{V_r} \left[C_1(n, V_r, \Lambda_b, \mu) \right] \right\} , \qquad (18)$$

The optimum toner intensity of the toner distribution Λ for each laser intensity V_r is selected from $\Lambda_b(n, Vr, \mu)$ with the optimum pair (n, μ) as

$$\Lambda_{opt}(V_r) = \Lambda_b(n_{opt}, V_r, \mu_{opt}) , \qquad (19)$$

Figure 5 shows the optimum Λ for various laser intensity V_r. As shown in Fig. 5, the intensity of the toner distribution Λ in the stochastic model increases as laser intensity increases. Figure 6 shows the simulated and measured mean reflectance of each printer addressable cell in the halftone screen with two laser intensity values $V_r = 1.0$ and 2.0 volts, respectively. The pixel cell in the halftone screen is indexed column-wised from the left to the right. It is evident from Fig. 6 that the proposed model can precisely predict reflectance of the halftone screen without any frequency modulation. Figure 7 shows the DFT of projected reflectance value for the predicted and the measured images embedded with 15 cycles/in and, respectively, 60 cycles/in sinusoidal intensity modulation with amplitude $\Delta V_r = 0.5$. In

Fig. 7, 75 cycle/in is the halftone screen frequency. As can be seen from Fig. 7, the proposed model is effective in predicting the printed reflectance due to embedding low spatial frequency intensity modulation. Majority of the frequency components and amplitudes match that of the measured reflectance data when the modulation frequency is as low as 15 cycles/in. However, the model is not as effective in predicting the reflectance impact associated with higher intensity modulation frequency, e.g. 60 cycle/in. This may result from the constrained bandwidth of the laser diode amplitude modulation system or the transient response of the scanner sensor array.
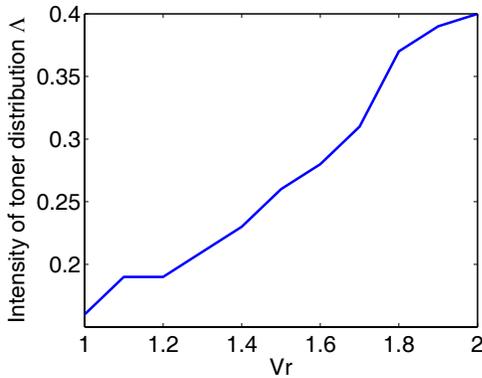

Figure 5. *Optimum intensity of toner distribution* Λ *for various reference voltages* V_r
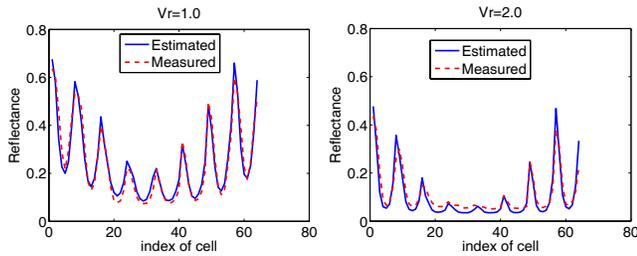

Figure 6. *Simulated and measured mean reflectance of each printer addressable pixel within the halftone screen printed with V_r = 1.0 and V_r = 2.0 volts*
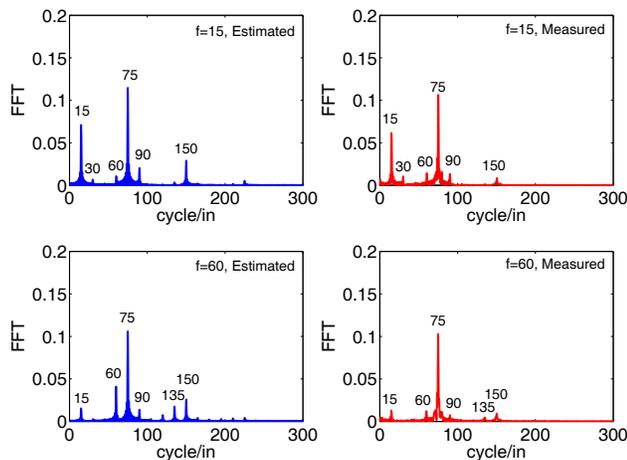

Figure 7. *DFT of Simulated and measured halftone image modulated with frequency 5 cycles/in and 60 cycles/in of sinusoidal wave*

Conclusions

In this paper, a stochastic dot interaction model is developed to predict the impact of embedding non-perceivable extrinsic signatures using laser intensity modulation. The model can be used to identify an optimal coding sequences and the associated decoding algorithm to maximize capacity and improve detection. The proposed model is effective for low embedding frequencies but illustrated some discrepancy between model and measurements when higher embedding frequency is used. Work is underway to investigate the discrepancy observed for higher embedding frequencies.

Acknowledgement

References

[1] P. J. Chiang, G. N. Ali, A. K. Mikkilineni, E. J. Delp, J. P. Allebach, and G. T.C. Chiu, "Extrinsic Signatures Embedding Using Exposure Modulation for Information Hiding and Secure Printing in Electrophotography", in Proceedings of the IS&T's NIP20: Int. Conf. On Digital Printing Technol., pp295-300

[2] A. K. Mikkilineni, P. J. Chiang, S. Suh, G. T.C. Chiu, J. P. Allebach and E. J. Delp, "Information Embedding and Extraction for Electrophotographic printing Processes", Proceedings of the SPIE Int. Conf. On Security, Steganography, and Watermarking of Multimedia Contents VIII, vol. 6072, p385-396, 2006.

[3] P. G. Roetling and T. M. Holladay, "Tone reproduction and screen design for pictorial electrographic printing," J. Appl. Photo. Eng., vol. 15, no.4, pp. 179–182, 1979.

[4] T. N. Pappas and D. L. Neuhoff, "Printer models and error diffusion," IEEE Trans. Image Processing, vol. 4, pp. 66-80, Jan. 1995.

[5] T. N. Pappas, C. Dong, and D. L. Neuhoff, "Measurement of printer parameters for model-based halftoning," J. Imag. Technol., vol. 2, no. 3, pp. 193–204, Jul. 1993.

[6] C. J. Rosenberg, "Measurement-based evaluation of a printer dot model for halftone algorithm tone correction," J. Imag. Technol., vol. 2, no. 3, pp. 205-212, July 1993.

[7] F. A. Baqai and J. P. Allebach, "Halftoning via direct binary search using analytical and stochastic printer models," IEEE Trans. Image Process, vol. 12, pp. 1–5, Jan. 2003.

[8] Q. Lin and J.Wiseman, "Impact of electrophotographic printer dot modeling on halftone image quality," in SID Int. Symp. Tech. Papers, Seattle, WA, May 1993, pp. 147–150.

[9] Q. Lin, "Screen design for printing," in Proc. IEEE Int. Conf. Image Processing, vol. II, Washington, DC, Oct. 1995, pp. 102-105.

[10] T. J. Flohr and J. P. Allebach, "Halftoning via direct binary search with a stochastic dot model," presented at the IS&T's 3rd Tech. Symp. Prepress, Proofing and Printing, Chicago, IL, Nov. 1993.

Author Biography

Pei-Ju Chiang received the B.S. degree in Mechanical and Marine Engineering from National Taiwan Ocean University, in 1999, and her M.S. degree in Mechanical Engineering from National Central University, in 2001. She is currently pursuing her Ph.D. degree in the School of Mechanical Engineering at Purdue University, West Lafayette. She is a student member of IS&T.